Degradation of microcystin-LR and cylindrospermopsin by continuous flow UV-A photocatalysis over immobilised TiO2.

CAMACHO-MUÑOZ, D., FERVERS, A.-S., PESTANA, C.J., EDWARDS, C. and LAWTON, L.A.

2020

Degradation of microcystin-LR and cylindrospermopsin by continuous flow UV-A photocatalysis over immobilised TiO_2

Dolores Camacho-Muñoz[a*], Anne-Sophie Fervers[a], Carlos J. Pestana[a], Christine Edwards[a], Linda A. Lawton[a]

[a]School of Pharmacy and Life Sciences, Robert Gordon University, Aberdeen, AB10 7GJ, UK

* Corresponding author email: l.camacho-munoz@rgu.ac.uk Tel. +44 (0) 1224 262871

Abstract

The increasing presence of freshwater toxins have brought new challenges to preserve water quality due to their potential impact on the environment and human health. Two commonly occurring cyanotoxins, microcystin-LR and cylindrospermopsin, with different physico-chemical properties were used to evaluate the efficiency of photocatalysis using a continuous-flow reactor with immobilized TiO_2 on glass tubes and UV-A light. The effect of flow rate and hydrogen peroxide addition on the efficiency of cyanotoxin removal were evaluated. An analysis of the effects on microcystin-LR removal efficiency showed that low flow rates (1mL/min) and high H_2O_2 concentrations (120 mg/L) were needed to provide effective degradation. Up to 27.9% and 39.1% removal of MC-LR and CYN, respectively were achieved by UV-A/TiO_2 after a single pass through the reactor. A slight increase of the removal of both cyanotoxins was observed when they were in a mixture (35.5% of MC-LR and 51.3% of CYN). The addition of H_2O_2 to the UV/TiO_2 system led to an average removal enhancement of 92.6% of MC-LR and of 29.5% of CYN compared to the UV/TiO_2 system. Photolysis assisted by H_2O_2 degraded MC-LR by up to 77.7%. No significant removal (<10%) was observed by photolysis alone or physical adsorption.

This study presents a proof-of-principle that demonstrates the feasibility for this technology to be integrated in large-scale applications.

Keywords: photocatalysis, cyanotoxin, hydrogen peroxide, immobilized titanium dioxide

1. Introduction

The ever-increasing global occurrence of cyanobacterial blooms have caused important damage to freshwater ecosystems (Scholz et al., 2017). Cyanobacteria are photosynthetic organisms that produce secondary metabolites of interest with important biological properties such as anti-inflammatory, antiviral, and anticancer activity among others (Demay et al., 2019). However, they also produce cyanotoxins as secondary metabolites that are linked to many human and animal poisoning events (Svirčev et al., 2019). The main route of human exposure of these cyanotoxins may occur through consumption of contaminated fish and vegetables irrigated with contaminated freshwater (Flores et al., 2018; Llana-Ruiz-Cabello et al., 2019; Mohamed and Bakr, 2018), or through ingestion of drinking water and during recreational use of water bodies with cyanobacterial blooms (Pineda-Mendoza et al., 2020; Svirčev et al., 2019).

According to their toxicological target, cyanotoxins are classified as hepatotoxins (liver), neurotoxins (nervous system), cytotoxins (several organs: liver, kidneys, small intestine, adrenal glands) and dermatotoxins (irritant toxins) (Wiegand and Pflugmacher, 2005). Of the various cyanotoxins, the hepatotoxin microcystins (MCs) are the most prevalent found in freshwater (Díez-Quijada et al., 2019; Scholz et al., 2017). To date, 246 MCs variants have been found (Spoof and Catherine, 2017) and there are significant differences in their toxicity and concentration in the environment (typically from a few µg/L to a few hundred µg/L) (Díez-Quijada et al., 2019). The most common and one of the most toxic congeners is the MC containing leucine and arginine (MC-LR) (PP2A IC_{50}: 0.032 nM; EC_{50}(72h): 2.63 mg/L to zebrafish embryos or larvae) (Ikehara et al., 2009; Wei et al., 2020).

Another prevalent problematic cyanotoxin is cylindrospermopsin (CYN). CYN is an alkaloid that contains a tricyclic guanidine moiety combined with a hydroxyl methyl uracil moiety and is highly soluble in water due to its zwitterionic nature (Chiswell et al., 1999). To date, 5 analogues are known (CYN, 7-epi-CYN, 7-deoxy-CYN, 7-deoxydesulfo-CYN and 7-deoxydesulfo-12-acetyl-CYN) (Kokociński et al., 2016). Environmental concentrations of CYN are usually in the range of 1-10 µg/L, but concentrations up to hundreds of µg/L have also been reported (De La Cruz et al., 2013; Rzymski and Poniedziałek, 2014).

MCs are released from the cells by lysis, ageing, and/or external stress factors (e.g. drinking water treatment) whereas high concentrations of CYN have been reported when cells are still viable in the water throughout the bloom event (Moura et al., 2018; Szlag et al., 2015). The World Health Organization proposes a recommended maximum allowable level in drinking water of 1 µg/L for MC-LR (WHO, 2011); and the Environmental Protection Agency of the

USA included MCs and CYN on their Contaminant Candidate List IV, with a 10-day health advisory of 1.6 µg/L for MCs and of 3 µg/L for CYN for adults (USEPA, 2015). Extracellular cyanotoxins and their metabolites are stable and are difficult to remove from water. Under natural environmental conditions, cyanotoxins can persist for long periods due to slow chemical and biological degradation and hence can enter drinking water plants which are not designed to deal with these contaminants (De La Cruz et al., 2013).

The advantages of TiO_2 as a photocatalyst for removing cyanotoxins from the aquatic environment in lab-scale and field-scale are well known; not only for water purification but also for detoxification (Antoniou et al., 2009; Feitz et al., 1999; Fotiou et al., 2015; Fotiou et al., 2013; Khedr et al., 2019; Liu et al., 2009; Liu et al., 2010; Pestana et al., 2020; Pinho et al., 2015a; Pinho et al., 2012; Sharma et al., 2012). TiO_2 is commonly used due to its high quantum efficiency, availability, low toxicity and chemical/physical stability. The working principle of TiO_2 photocatalytic systems involve the production of electron (e_{cb}^-)/hole (h_{vb}^+) pairs upon UV illumination (higher than the energy band gap for the two TiO_2 crystalline forms that show photocatalytic activity: anatase 3.2 eV and rutile 3.0 eV) and the formation of reactive oxidant species (ROS) as a result (hydroxyl radicals, $OH^{\cdot}$ and superoxide radical anions, $O_2^{\cdot -}$).

According to the literature, a high number of studies report the use of batch systems where TiO_2 nanoparticles are suspended in the liquid phase and because of their large surface area is beneficial for mass transfer (Lawton et al., 1999). However, suspended TiO_2 particles also present mayor drawbacks: i) additional costly step to recover the photocatalyst particles from the liquid phase; ii) light scattering; iii) formation of photocatalyst aggregates. Therefore, the immobilization of TiO_2 on a large variety of supporting materials (e.g. glass beads, silica-based materials, biomass, activated carbon, membranes, clay) has been explored (Srikanth et al., 2017; Xing et al., 2018).

In this study, we evaluate the performance of a UV/TiO_2 system with and without the presence of an oxidant to degrade/mineralize cyanotoxins in artificial freshwater (AFW) using a lab-scale continuous-flow reactor with TiO_2-coated glass tubes in a single pass. Two model cyanotoxins ubiquitous in freshwater, MC-LR and CYN, with different physico-chemical properties in single and mixed solutions were used. The performance of the reactor was evaluated regarding the flow rate and different concentrations of the oxidant H_2O_2. To get a better insight regarding the interaction between the cyanotoxins and UV-A, TiO_2 and H_2O_2, photolysis (UV-A) and physical adsorption (non-irradiated TiO_2) with and without H_2O_2 as well as chemical oxidation by H_2O_2 were also evaluated.

2. Materials and methods

2.1 Chemicals and reagents

HPLC grade methanol, acetonitrile and trifluoroacetic acid were purchased from Sigma-Aldrich (Irvine, UK). Ultrapure water (18.2 MΩ.cm) was provided by a PURELAB flex system (ELGA LabWater, Veolia Water Technologies, Germany). H_2O_2, $CaCl_2$, $MgSO_4$, $NaHCO_3$, KCl, Na_2HPO_4, NaH_2PO_4, N,N-diethyl-1,4-phenylenediammonium sulphate (DPD), H_2SO_4, horseradish peroxidase (HRP) (Type II, 181 purpurogallin units/mg) were obtained from Sigma-Aldrich. Artificial freshwater (AFW) was prepared as described by Akkanen and Kukkonen (2003). Briefly, $CaCl_2$ (58.5 mg/L), $MgSO_4$ (24.7 mg/L), $NaHCO_3$ (13 mg/L) and KCl (1.2 mg/L) were dissolved in ultrapure water and adjusted to pH 7. MC-LR (≥95%) from *Microcystis aeruginosa* and CYN (≥95%) from *Cylindrospermopsis raciborskii* were isolated in-house (Fig. S1). Stock and working solutions were prepared in AFW.

2.2 Reactor design

The lab-scale continuous-flow reactor used in this study was previously described (Adams et al., 2013; Gbadamosi, 2019). The schematic diagram of the experimental reactor setup is shown in Fig. S2. The cylindrical reactor vessel was made of clear glass with stainless steel end-fittings (height 150 mm, internal diameter 31.8 mm, wall thickness 9.1 mm, volume 84 mL). Inside the reactor, 30 glass tubes (0.5 cm diameter) were coated with TiO_2 (0.96%) by a modified sol-gel method described by Islam et al. (2016). Uncoated glass tubes were used for experimental controls (UV-A, H_2O_2, UV-A/H_2O_2) (Table S1).

2.3 Experimental set-up

Photocatalysis experiments were conducted in a lab-scale flow through immobilized photocatalytic reactor (FTIPR) equipped with 4 UV-A lamps (Philips PL-L 36W/09/4P UV-A; wavelength 315-380 nm) in an illumination box designed by Skillen et al. (2016). The design consisted of a sample feed-in system, photocatalysis reactor and sampling points (Fig. S2).

Initially, factors influencing reaction such as flow rate and oxidant concentration were optimized. The effect of flow rate (1 and 5 mL/min) and the addition of H_2O_2 (0, 6, 30, 60, 120 and 240 mg/L) using MC-LR as a model were investigated. Experiments were done in triplicate. To study the effect of the flow rate a MC-LR solution (3 µg/mL) was flushed

through the reactor via an inlet tube at the bottom of the reactor using a peristaltic pump at 1 and 5 mL/min. An aliquot (1 mL) was taken after one reactor volume (RV) (residence time: 84 min at 1 mL/min and 16.8 min at 5 mL/min) was passed through the reactor from a tube located at the bottom of the reactor, then the UV-A lamp was switched on and another sample was collected (1 mL) after one RV was passed through the reactor. The system was flushed with 2 RV of AFW with UV-A irradiation in between the experiments (Fig. S3). Samples were analysed by high performance liquid chromatography with photodiode array detection (HPLC-PDA). To study the effect of H_2O_2 different concentrations of H_2O_2 were added to a MC-LR solution (3 µg/mL), flushed at 1 mL/min through the reactor with UV-A irradiation and aliquots (1.5 mL) collected after 84, 104, 124, 144 and 164 min. System was flushed with 3 RV of AFW at 5 mL/min with UV-A irradiation in between the experiments (Fig. S4). Samples were analysed by HPLC-PDA for cyanotoxins (section 2.5) and UV-Vis spectrophotometry for H_2O_2 (section 2.6).

A solution of AFW containing 3 µg/mL of MC-LR, 3 µg/mL of CYN or a mixed solution of 1.5 µg/mL of MC-LR and CYN each was channelled through the FTIPR using a peristatic pump at 1 mL/min. Samples were taken at 84, 104, 124, 144 and 164 min and analysed by HPLC-PDA and spectrophotometric analysis. Experiments were run in triplicate under each of these different conditions: presence and absence of photocatalyst (TiO_2, 1%), oxidant (H_2O_2, 120 mg/L) and UV-A light (Table S1).

2.4 Analysis by HPLC-PDA

The quantification of MC-LR and CYN was performed by High-Performance Liquid Chromatography (HPLC) using Waters Alliance 2695 solvent delivery system (Waters, UK) equipped with a Waters 2996 photodiode array detector (PDA) for MC-LR analysis and with a Waters 996 PDA for CYN analysis.

MC-LR separation was carried out on a C18 Waters Symmetry column (150 x 2.1 mm, 5 µm particle size) at 40°C. Ultrapure water (A) and acetonitrile (B) both containing 0.05% trifluoroacetic acid constituted the mobile phase. MC-LR was separated using a linear gradient increasing from 20% to 70% B at flow rate of 0.3 mL/min over 25 min, followed by an organic solvent wash (100% B) and re-establishment of starting conditions for the next 10 min. CYN separation was performed on a C18 Waters Atlantis column (150 x 2.1 mm, 5 µm particle size) at 40ºC. CYN was separated using a gradient elution with ultrapure water (A) and methanol (B) as mobile phase starting at 2% B and increasing to 25% B at 0.3 mL/min

over 25 min, followed by an organic wash (100% B) and re-equilibration for the next 5 min. Injection volume was 20 µL for MC-LR and 10 µL for CYN.
The PDA acquisition wavelength was set in the range of 200-400 nm at 1.2 nm resolution. MC-LR was monitored at 238 nm and CYN at 262 nm. Limit of quantification was 0.1 µg/mL for MC-LR and CYN, respectively.
Quantification was carried out by external calibration over the range 0.1-25 µg/mL. Chromatographic data was acquired and processed using Empower software v 2.0 (Waters, UK) for MC-LR and using MassLynx software v 4.1 (Waters, UK) for CYN.

2.5 Analysis of H_2O_2 by spectrophotometry

H_2O_2 concentrations were analysed using a spectrophotometrical method as described by Fan et al. (2013). Briefly, buffer stock solutions (pH 6) were prepared by mixing 0.5 M Na_2HPO_4 and 0.5 M NaH_2PO_4. Sample (40 µL) was mixed with 100 µL of buffer, 40 µL of DPD (0.1 g of N,N-diethyl-1,4-phenlenediammonium sulphate in 10 mL of 0.1N H_2SO_4), 10 µL of HRP (10 mg of horseradish peroxidase Type II, 181 purpurogallin units/mg in 10 mL of deionized water) and 0.9 mL of ultrapure water in a 1 cm path-length optical cuvette. Colorimetric analysis was performed using an UV/Vis spectrophotometer (Thermo Scientific, UK) at a wavelength of 551 nm. A calibration curve was prepared ranging from 0 to 10 mg/L.

3. Results and discussion

3.1 Optimization of flow rate for cyanotoxin removal in a FTIPR

Flow rate plays an important role in continuous flow reactors due to its direct impact on residence time. The effect of flow rate on the photocatalytic oxidation of a model cyanotoxin (MC-LR, 3 µg/mL) was investigated at 1 and 5 mL/min (Fig. 1). The TiO_2 coated glass tubes were closely packed in the reactor vessel in order to increase the mass transfer between the surface of the immobilized catalyst and the cyanotoxin.
It can be seen from Fig. 1 that in the absence of UV-A light, no significant differences were observed in the removal of MC-LR due to physical adsorption at 1 mL/min (9.0%) and 5 mL/min (11.9%). On the other hand, under UV-A irradiation an increase in the flow rate resulted in low removal rate due to a lower time for reaction. At flow rate of 1 mL/min (residence time 84 min) MC-LR was removed up to 24.9% in a single pass whereas at 5 mL/min (residence time 16.8 min) the removal of MC-LR decreased to 3.9%.
This effect is a typical behaviour of continuous flow reactors. At lower flow rates, there is more time for reaction as the contact time between the immobilized photocatalyst and the

pollutant is greater than at higher flow rates. As a result, residence time has a great impact on the kinetics of the reaction (Damodar and Swaminathan, 2008; Rezaei et al., 2014). Catalyst surface area exposed to UV irradiation and flow rate were identified as crucial factors for MC-LR removal in a simple packed bed flow reactor with pelletised TiO_2 (Liu et al., 2009). The lower flow (1 mL/min) was used for further experiments.

3.2 Optimization of H_2O_2 concentration for cyanotoxin removal in a FTIPR

Dissolved oxygen is a limiting factor for TiO_2 photocatalysis (Pelaez et al., 2011). The continuous flow reactor is an enclosed vessel; therefore the addition of oxidants is beneficial for the photooxidation of the cyanotoxin. H_2O_2 is a strong oxidant widely used in advanced oxidation processes that act as both hydroxyl radical source and electron-hole recombination inhibitor. The oxidation efficiency of the system is limited by the production of hydroxyl radicals ($OH^{\cdot}$), which increases by increasing the oxidant content, until an excessive high content of the oxidant hinders the oxidation process (Cornish et al., 2000; He et al., 2012; Sahel et al., 2016).

Therefore, it is necessary to find the optimal oxidant concentration to get the maximum oxidation efficiency for a model cyanotoxin (MC-LR). Fig.2 shows that concentrations of H_2O_2 up to 30 mg/L did not improve removal of MC-LR whereas increasing concentrations of H_2O_2 (from 60 mg/L up to 240 mg/L) influenced positively the degradation of MC-LR up to 58.0% in a single pass. In this study, no detrimental effect on the oxidation process was observed at the highest H_2O_2 concentration tested (240 mg/L) as it was described in previous reports (Li et al., 2009).

However, the residual H_2O_2 concentration in the photocatalytic system must also be considered. Removal of H_2O_2 was in the range 96.0-98.5% in all the H_2O_2 concentrations tested after a single pass. Although most of H_2O_2 was removed from the system, >96.0% of removal meant mean residual concentrations of H_2O_2 of 0.18, 0.68, 1.09, 1.75 and 9.6 mg/L using initial H_2O_2 concentrations of 6, 30, 60, 120 and 240 mg/L, respectively. It is well known that the toxicity of H_2O_2 is dependent on its concentration (reported toxicity values: 16.4 mg/L LC_{50} (96h) fish (*Pimephales promelas*), 2.4 mg/L EC_{50} (24h) invertebrate (*Daphnia pulex*), 0.63 mg/L NOEC (21d) invertebrate (*Daphnia magna*), 0.63 mg/L NOEC (72h) algae (*Skeletonema costatum*) (European Chemical Agency) (ECHA).

For further experiments 120 mg/L of H_2O_2 were used as it represented the best compromise between removal efficiency of MC-LR and content of residual H_2O_2.

3.3 UV-A/TiO_2 photocatalysis for MC-LR and CYN removal

Concentrations of MC-LR and CYN in the aquatic environment can range from a few to a few hundreds µg/L (De La Cruz et al., 2013; Díez-Quijada et al., 2019) representing a serious environmental and health issue. The efficiency of the photocatalytic process to remove MC-LR and CYN in single and mixed solutions in AFW using a FTIPR in a single pass was evaluated (Fig. 3A-F). To obtain a better insight regarding the interactions between UV-A, TiO_2 and the toxins, photolysis (UV-A) and physical adsorption (non-irradiated TiO_2) treatments were performed keeping the same operational parameters as of the UV-A/TiO_2 photocatalysis process.

The effect of UV-A irradiation in the absence of the catalyst on the removal of MC-LR and CYN is illustrated in Fig. 3A and B. Under UV-A light, degradation of MC-LR and CYN was low, 3% of MC-LR was removed after 84 min and no change in degradation was observed whereas degradation of CYN fluctuated (2.9-7.0%) during the experiment (Fig. 3A). Similar low removals were observed in the mixed toxin solution (MC-LR 4.9-7.1% and CYN 3.5-4.9%) (Fig. 3B). In line with previous studies, irradiation alone (UV, visible and solar) is not effective to degrade MC-LR and CYN (Antoniou et al., 2009; Chen et al., 2015; Feitz et al., 1999; Fotiou et al., 2015; Khedr et al., 2019; Lawton et al., 1999; Lawton et al., 2003; Liu et al., 2010; Pinho et al., 2015a; Pinho et al., 2012).

At pH 7, CYN (pKa 8.8), MC-LR (pka 2.09, 2.19 and 12.48) and surface of TiO_2 (point of zero charge is pH 6.5) are in neutral or slightly negatively charged state so adsorption capacity is very low. The extent to which MC-LR and CYN are adsorbed on the surface of the catalyst is shown in Fig. 3D and E. In the absence of UV-A light, physical adsorption followed a typical trend in which only 5.4% MC-LR and 6.2% of CYN were removed after 84 min and then removal decreased gradually over time, faster for MC-LR (<0.5% after 104 min) than for CYN (<5% after 104 min) (Fig. 3D). A similar trend but less evident was observed for the mixed toxin solution (5.9% and 6.4% after 84 min and 1.4% and 3.3% after 164 min for MC-LR and CYN, respectively (Fig. 3E)). Overall, the number of molecules per min passing through the photocatalytic reactor did not differ greatly between experiments (MC-LR: 1.93×10^{15} molecules/min, CYN: 3.76×10^{15} molecules/min and in the mixed MC-LR/CYN solution: 9.07×10^{14} molecules/min of MC-LR and 1.88×10^{15} molecules/min of CYN). However, there are significant differences in the size and hydrophilic/hydrophobic interactions of MC-LR and CYN that could explain the differences observed (Fig. 3D). MC-LR is relatively larger (995.172 Da), more bulky and slightly less hydrophilic than CYN which is smaller (415.422 Da) (Fig. S1). This could limit the adsorption capacity and saturate

the active sites of the catalyst. For example, Feitz et al. (1999) reported that one MC-LR molecule could occupy up to 5 active sites of TiO_2 due to its size and 3D structure.

Direct comparison with previous studies is difficult as operational parameters vary greatly and therefore influence results. However, previous studies reported low physical adsorption of MC-LR and CYN in TiO_2 solution (Chen et al., 2015; Pinho et al., 2015a; Yang et al., 2020) and immobilized TiO_2 (<10%) (Pestana et al., 2020; Pinho et al., 2015b).

The efficiency of UV-A/TiO_2 is based on the generation of highly reactive oxygen species (e.g. $OH^{\cdot}$, $O_2^{\cdot -}$) upon irradiation with energy equal to or greater than the TiO_2 band gap. The combination of UV-A and TiO_2 enhanced the degradation of MC-LR and CYN as shown in Fig. 3E and F. Degradation of MC-LR was in the range 23.2-27.9% and of CYN in the range of 36.4-39.1% (Fig. 3E) after a single pass. Removal rate of MC-LR increased 7.1% and CYN 11.7% when the toxins were present in a mixture (29.9-35.5% for MC-LR and 47.6-51.3% for CYN) (Fig. 3F). These removal values are due to photocatalysis essentially as photolysis and physical adsorption were low (<7.1%). Under UV irradiation changes on the electric properties of TiO_2 surface occur, altering the adsorption sites of the catalyst (Xu and Langford, 2000).

Detailed studies concerning the reaction pathways for the degradation of MC-LR (Antoniou et al., 2008; Liu et al., 2003; Yang et al., 2020) and CYN (Chen et al., 2015; Fotiou et al., 2015; Zhang et al., 2015) using UV-A/TiO_2 have been previously performed. Based on previous LC-MS data (Liu et al., 2009; Liu et al., 2003) the breakdown mechanism of MC-LR involved an initial photoisomerisation of the MC, hydroxyl radical attack, cleavage of the Adda conjugated diene structure and cleavage of the Mdha double bond with subsequent residue oxidation and peptide bond hydrolysis. Regarding CYN degradation the proposed pathway is based on hydroxylation, sulfate elimination and ring opening on the hydroxymethyl uracil moiety and tricyclic guanidine moiety by hydroxyl radical attack (Zhang et al., 2015).

Previous reports have shown that the fastest degradation rate of MC-LR was achieved under acidic conditions. At acidic pH high electrostatic attractive forces arise between $TiOH_2^+$ and $MC\text{-}LRH^-$, then oxidizing species (OH* and $O_2{}^{*-}$) generated on the surface of the catalyst efficiently degraded MC-LR (Antoniou et al., 2009; Pelaez et al., 2011; Yang et al., 2020). On the other hand, at neutral pH the electrostatic forces are weaker or negligible and thin and thick TiO_2 films showed similar reaction rate constants (Antoniou et al., 2009). Moreover, acidification/neutralization steps in a full-scale water treatment plant are not cost-effective.

3.4 H_2O_2 assisted UV-A/TiO_2 photocatalysis for MC-LR and CYN removal

Dissolved oxygen is a limiting factor for TiO_2 photocatalysis (Pelaez et al., 2011). In this study the continuous-flow reactor vessel is enclosed and the addition of H_2O_2 is able to serve as an oxygen source to improve the photocatalytic process. The effect of H_2O_2 on the oxidation of both cyanotoxins, on photolysis (UV-A/H_2O_2), on physical adsorption (TiO_2/H_2O_2) and on the photocatalytic process (UV-A/TiO_2/H_2O_2) was evaluated (Fig. 4A-H).

Firstly, MC-LR and CYN were exposed to H_2O_2 (120 mg/L) and the effects in terms of degradation were evaluated (Fig. 4A and B). Chemical oxidation by H_2O_2 greatly affected the removal of MC-LR which gradually increased over time from 15.6% at 84 min to 30.2% at 164 min. This effect was not observed for CYN which removal fluctuated between 3.0 and 7.6%. However, in the mixture of toxins removal rates of MC-LR (4.0-9.6%) and CYN (5.4-10.5%) were steady over time. Previous studies that used concentrations of H_2O_2 up to 68 mg/L found that H_2O_2 is not able to effectively degrade MCs (He et al., 2012; Li et al., 2009) but in this study 120 mg/L of H_2O_2 removed MC-LR which was positively correlated with the contact time.

Then, degradation of MC-LR and CYN by the UV-A/H_2O_2 system was evaluated (Fig. 4C and D). The combination of H_2O_2 and UV-A resulted to be the most favourable for the removal of MC-LR 77.7% (Fig. 4C). However, when the toxins were combined removal of MC-LR decreased up to 47.5% whereas removal of CYN (32.2%) did not seem to be affected by the presence of MC-LR (Fig. 4D). The UV-A/H_2O_2 process involves a single-step dissociation of the oxidant to form two $OH^{\cdot}$ which can oxidize the toxins non-selectively:

$$H_2O_2 + hv \rightarrow 2OH^{\cdot}$$

$OH^{\cdot}$ attack, oxidation and UV direct photolysis are the main mechanisms involved in MC-LR degradation by UV/H_2O_2 according to Liu et al. (2016). They also pointed out that the $OH^{\cdot}$ attacks the conjugated diene bond, benzene ring and methoxy group of the Adda side chain of MC-LR (Liu et al., 2016). He et al. (2014) revealed that hydroxylation by $OH^{\cdot}$ attack is the main reaction pathway to degrade CYN in the UV/H_2O_2 system and it involves the hydroxylation and cleavage of the uracil ring, the oxidation of the secondary alcohol to carbonyl and the loss of the sulphate group.

UV/H_2O_2 has been widely studied and used to degrade cyanotoxins in water (He et al., 2012; He et al., 2014; Li et al., 2009; Liu et al., 2016). High degradation of MC-LR has been linked to increasing H_2O_2 concentration (up to 102 mg/L), neutral and acidic conditions and low concentrations of anions (CO_3^{2-}, NO_3^-) (Li et al., 2009). The presence of anions typically

found in natural water affects the UV/H_2O_2 performance. CO_3^{2-} and NO_3^- are well known $OH^\cdot$ scavengers whereas Cl^- and SO_4^{2-} have shown a negligible inhibiting effect in the UV/H_2O_2 systems (Li et al., 2009). In this study the concentration of anions were 20-100 times lower than the ones reported by Li et al. (2009), therefore their effect was considered negligible. However, removal of H_2O_2 was low <8.3% and therefore it is not a suitable treatment for toxin removal. In fact, photolysis of H_2O_2 needs radiation below 280 nm for an effective H_2O_2 decomposition (Pignatello et al., 2006).

Next, the TiO_2/H_2O_2 system was evaluated (Fig. 4E and F). The combination of TiO_2 and H_2O_2 (no UV-A irradiation) achieved low removals of the single (1.6-6.7%) and mixed toxins (3.0-9.0%) Fig. 4E and F. These values were similar to the ones achieved by physical adsorption on TiO_2 (<6.4% for MC-LR and CYN) but lower than the ones obtained by chemical oxidation with H_2O_2, especially for MC-LR (<30.2%). The presence of H_2O_2 affected the adsorption of MC-LR on the surface of TiO_2. This decrease on the photocatalytic degradation of MC-LR could be due to the competition between MC-LR and H_2O_2 for the surface sites of TiO_2 (Cornish et al., 2000). H_2O_2 can be adsorbed onto the surface of TiO_2 modifying the surface of the catalyst and subsequently decreasing its catalytic activity (Cornish et al., 2000). As result, the removal of H_2O_2 was 14.3% after 84 min and then decreased gradually over time to 8.3% after 164 min as the adsorption process reached equilibrium. The adsorption and degradation of H_2O_2 on different commercial TiO_2 sample were studied by Sahel et al. (2016). The adsorption capacity of H_2O_2 depended on the structure of TiO_2 and on OH surface density and it was characterized by the Langmuir model (Sahel et al., 2016).

Finally, removal of MC-LR and CYN by the combined UV-A/TiO_2/H_2O_2 photocatalytic process is shown in Fig. 4G and H. Degradation was steady over time and similar results were obtained with the single and the mixed toxin solutions. Mean removal rate of MC-LR and CYN were 49.3% and 48.9%, respectively; and in mixed solution: 40.7% and 47.9%, respectively. UV-A/TiO_2/H_2O_2 system led to an average removal increment of 92.6% of MC-LR and of 29.5% of CYN in comparison with the ones obtained in the UV-A/TiO_2 treatment. UV-A/TiO_2/H_2O_2 system increased by 2-fold the removal of MC-LR in the UV-A/TiO_2 system (25.6%) but did not reach the efficient removal obtained in the UV-A/H_2O_2 system (77.7%). Cornish et al. (2000) showed that the addition of H_2O_2 displaced the pre-adsorbed MC-LR molecules onto the illuminated TiO_2 surface suggesting a strong competition between the MC-LR molecules and H_2O_2 for active sites on the TiO_2 surface. They found a

corresponding enhancement in the removal of MC-LR as the concentration of H_2O_2 was reduced from 0.6% to 0.1% (v/v).

Maximum removal of H_2O_2 (96.5-98.5%) was achieved in this system (UV-A/TiO_2/H_2O_2) and it was due to the photocatalytic process as direct photolysis of H_2O_2 at the UV-A wavelength used (315-380 nm) was negligible as shown previously. The surface area of the TiO_2 and the amount of H_2O_2 adsorbed play a role on the degradation under UV irradiation that takes place on the surface but also near the surface of the catalyst (Sahel et al., 2016).

3.5 Future perspectives for the application of continuous flow reactors with immobilized TiO_2

Continuous-flow photocatalytic reactors have become the most promising and practical technology for water treatment. In comparison with batch systems, a continuous-flow reactor brings great advantages in terms of efficiency, sustainability and safety. The continuous-flow reactor with immobilized TiO_2 and UV-A radiation source used in this study represents a significant step towards the implementation of this technology in water treatment applications.

The use of immobilized TiO_2 as an alternative to suspended TiO_2 eliminate the additional post-treatment separation, reduce or eliminate the scattering of light and the aggregation of catalytic particles and enhance the reusability of the photocatalyst as well as allows continuous operation of the reactor. However, a partial or total blockage of the active sites of the immobilized photocatalyst is also a possibility. Support materials come with inherent advantages and disadvantages. In this study, TiO_2 coated on glass tubes were tightly packed minimizing mass transfer limitations, maximizing surface area per unit of volume and light penetration and increasing contact of the sample and the photocatalyst. This support design resulted in removals of up to 49.3% of MC-LR and 48.9% of CYN using UV-A/TiO_2/H_2O_2 system in a single pass. A recent study showed the potential of a reactor packed with TiO_2 coated glass beads which could be deployed in water reservoirs and run continuously to remove microcystins (Gunaratne et al., 2020).

Many studies evaluate the performance of photocatalysts rather than explore different reactor configurations. The reactor configuration used in this study could be easily scaled up by increasing the path length and/or the diameter. Moreover, it allows for the connection of several reactors in series, in parallel and use it in recirculation mode what would increase the removals of cyanotoxins achieved by the current reactor configuration in a single pass.

The ultimate aim of photocatalysis is to use low cost energy/radiation sources. Challenges remain to optimize photocatalysts with a wide absorption light wavelength that could use solar, visible and infrared radiation. UV-LEDs are an environmental safe technology option as they could be used in mobile devices maintained by batteries or solar cells. This study used UV-A lamps but with the current reactor configuration they could be easily replaced by UV-LED strips as showed in a previous study (Gunaratne et al., 2020).

4. Conclusions

The presence of cyanotoxins in the aquatic environment is an issue of major concern due to the detrimental effects that they may have on the environment and human health. The present study revealed that UV-A/TiO_2/H_2O_2 is an efficient technology to degrade two model cyanotoxins: MC-LR and CYN in a continuous-flow reactor with immobilized TiO_2 in a single pass. Addition of H_2O_2 benefited the removal of MC-LR and CYN in the photocatalytic system. These findings are a useful contribution to improve the effectiveness of advanced oxidation processes on cyanotoxin removal.

In addition, this study presents a proof-of-principle that demonstrate the feasibility for this technology to be integrated in large-scale applications. The continuous-flow reactor with coated TiO_2 glass tubes presents the advantage of no need of post-treatment catalyst separation. The arrangement of the TiO_2 coated glass tubes and the configuration of the reactor allow for future development of large-scale photocatalytic reactors by increasing the path length and the diameter of the reactor.

Acknowledgments

The authors would like to acknowledge the Engineering and Physical Sciences Research Council (EPSRC) [EP/P029280/1] and the Biotechnology and Biological Sciences Research Council (BBSRC) [BB/S004211/1] for funding this research. As per EPSRC requirements, the data will be made publicly available on the Robert Gordon University's repository, OpenAIR@RGU. Len Montgomery is appreciated for proof-reading the manuscript.

Conflict of interest

The authors declare no conflict of interests.

References

Adams, M., Skillen, N., McCullagh, C., Robertson, P.K.J., 2013. Development of a doped titania immobilised thin film multi tubular photoreactor. Appl. Catal. B: Environ. 130–131, 99–105.

Akkanen, J., Kukkonen, J.V.K., 2003. Biotransformation and bioconcentration of pyrene in *Daphnia magna*. Aquat. Toxicol. 64, 53–61.

Antoniou, M.G., Nicolaou, P.A., Shoemaker, J.A., De la Cruz, A.A., Dionysiou, D.D., 2009. Impact of the morphological properties of thin TiO_2 photocatalytic films on the detoxification of water contaminated with the cyanotoxin, microcystin–LR. Appl. Catal. B: Environ. 91, 165–173.

Antoniou, M.G., Shoemaker, J.A., De la Cruz, A.A., Dionysiou, D.D., 2008. Unveiling New Degradation Intermediates/Pathways from the Photocatalytic Degradation of Microcystin–LR. Environ. Sci. Technol. 42, 8877–8883.

Chen, L., Zhao, C., Dionysiou, D.D., O'Shea, K.E., 2015. TiO_2 photocatalytic degradation and detoxification of cylindrospermopsin. J. Photochem. Photobiol. A: Chem. 307–308, 115–122.

Chiswell, R.K., Shaw, G.R., Eaglesham, G., Smith, M.J., Norris, R.L., Seawright, A.A., Moore, M.R., 1999. Stability of cylindrospermopsin, the toxin from the cyanobacterium, *cylindrospermopsis raciborskii*: Effect of pH, temperature, and sunlight on decomposition. Environ. Toxicol. 14, 155–161.

Cornish, B.J.P.A., Lawton, L.A., Robertson, P.K.J., 2000. Hydrogen peroxide enhanced photocatalytic oxidation of microcystin–LR using titanium dioxide. Appl. Catal. B: Environ. 25, 59–67.

Damodar, R.A., Swaminathan, T., 2008. Performance evaluation of a continuous flow immobilized rotating tube photocatalytic reactor (IRTPR) immobilized with TiO_2 catalyst for azo dye degradation. Chem. Eng. J. 144, 59–66.

De La Cruz, A.A., Hiskia, A., Kaloudis, T., Chernoff, N., Hill, D., Antoniou, M.G., He, X., Loftin, K., O'Shea, K., Zhao, C., Peláez, M., Han, C., Lynch, T.J., Dionysiou, D.D., 2013. A review on cylindrospermopsin: The global occurrence, detection, toxicity and degradation of a potent cyanotoxin. Environ. Sci.: Process. Impacts 15, 1979–2003.

Demay, J., Bernard, C., Reinhardt, A., Marie, B., 2019. Natural Products from Cyanobacteria: Focus on Beneficial Activities. Mar. Drugs 17, 320.

Díez–Quijada, L., Prieto, A.I., Guzmán–Guillén, R., Jos, A., Cameán, A.M., 2019. Occurrence and toxicity of microcystin congeners other than MC–LR and MC–RR: A review. Food Chem. Toxicol. 125, 106–132.

ECHA (https://echa.europa.eu/registration-dossier/-/registered-dossier/15701/6/2/5; accessed 04 June 2020)

Fan, J., Ho, L., Hobson, P., Brookes, J., 2013. Evaluating the effectiveness of copper sulphate, chlorine, potassium permanganate, hydrogen peroxide and ozone on cyanobacterial cell integrity. Water Res. 47, 5153–5164.

Feitz, A.J., Waite, T.D., Jones, G.J., Boyden, B.H., Orr, P.T., 1999. Photocatalytic Degradation of the Blue Green Algal Toxin Microcystin–LR in a Natural Organic–Aqueous Matrix. Environ. Sci. Technol. 33, 243–249.

Flores, N.M., Miller, T.R., Stockwell, J.D., 2018. A Global Analysis of the Relationship between Concentrations of Microcystins in Water and Fish. Front. Mar. Sci. 5.

Fotiou, T., Triantis, T., Kaloudis, T., Hiskia, A., 2015. Photocatalytic degradation of cylindrospermopsin under UV–A, solar and visible light using TiO_2. Mineralization and intermediate products. Chemosphere 119, S89–S94.

Fotiou, T., Triantis, T.M., Kaloudis, T., Pastrana–Martínez, L.M., Likodimos, V., Falaras, P., Silva, A.M.T., Hiskia, A., 2013. Photocatalytic Degradation of Microcystin–LR and Off–Odor Compounds in Water under UV–A and Solar Light with a Nanostructured Photocatalyst Based on Reduced Graphene Oxide–TiO_2 Composite. Identification of Intermediate Products. Ind. Eng. Chem. Res. 52, 13991–14000.

Gbadamosi, T.G., 2019. Development of a novel photocatalytic reactor for the treatment of polycyclic aromatic hydrocarbons. Thesis. Robert Gordon University, UK.

Gunaratne, H.Q.N., Pestana, C.J., Skillen, N., Hui, J., Saravanan, S., Edwards, C., Irvine, J.T.S., Robertson, P.K.J., Lawton, L.A., 2020. 'All in one' photo–reactor pod containing TiO_2 coated glass

491 beads and LEDs for continuous photocatalytic destruction of cyanotoxins in water. Environ. Sci.
492 Water Res. Technol. 6, 945–950.
493 He, X., Pelaez, M., Westrick, J.A., O'Shea, K.E., Hiskia, A., Triantis, T., Kaloudis, T., Stefan, M.I.,
494 de la Cruz, A.A., Dionysiou, D.D., 2012. Efficient removal of microcystin–LR by UV–C/H_2O_2 in
495 synthetic and natural water samples. Water Res. 46, 1501–1510.
496 He, X., Zhang, G., De La Cruz, A.A., O'Shea, K.E., Dionysiou, D.D., 2014. Degradation mechanism
497 of cyanobacterial toxin cylindrospermopsin by hydroxyl radicals in homogeneous UV/H_2O_2
498 process. Environ. Sci. Technol. 48, 4495–4504.
499 Ikehara, T., Imamura, S., Sano, T., Nakashima, J., Kuniyoshi, K., Oshiro, N., Yoshimoto, M.,
500 Yasumoto, T., 2009. The effect of structural variation in 21 microcystins on their inhibition of
501 PP2A and the effect of replacing cys269 with glycine. Toxicon 54, 539–544.
502 Islam, S., Bidin, N., Riaz, S., Krishnan, G., Daud, S., Naseem, S., Marsin, F.M., 2016. Sol–gel based
503 optically active phenolphthalein encapsulated nanomatrices for sensing application. J. Sol–Gel Sci.
504 Technol. 79, 616–627.
505 Khedr, T.M., El–Sheikh, S.M., Ismail, A.A., Kowalska, E., Bahnemann, D.W., 2019.
506 Photodegradation of Microcystin–LR Using Visible Light–Activated C/N–co–Modified
507 Mesoporous TiO_2 Photocatalyst. Materials 12, 1027.
508 Kokociński, M., Cameán, A.M., Carmeli, S., Guzmán–Guillén, R., Jos, Á., Mankiewicz–Boczek, J.,
509 Metcalf, J.S., Moreno, I.M., Prieto, A.I., Sukenik, A., 2016. Cylindrospermopsin and congeners,
510 in: Meriluoto, J., Spoof, L., Codd, G.A. (Eds.), Handbook of Cyanobacterial Monitoring and
511 Cyanotoxin Analysis. John Wiley & Sons, Ltd.
512 Lawton, L.A., Robertson, P.K.J., Cornish, B.J.P.A., Jaspars, M., 1999. Detoxification of Microcystins
513 (Cyanobacterial Hepatotoxins) Using TiO_2 Photocatalytic Oxidation. Environ. Sci. Technol. 33, 771–
514 775.
515 Lawton, L.A., Robertson, P.K.J., Cornish, B.J.P.A., Marr, I.L., Jaspars, M., 2003. Processes
516 influencing surface interaction and photocatalytic destruction of microcystins on titanium dioxide
517 photocatalysts. J. Catal. 213, 109–113.
518 Li, L., Gao, N.–Y., Deng, Y., Yao, J.–J., Zhang, K.–J., Li, H.–J., Yin, D.–D., Ou, H.–S., Guo, J.–W.,
519 2009. Experimental and model comparisons of H_2O_2 assisted UV photodegradation of
520 Microcystin–LR in simulated drinking water. J. Zhejiang University–SCIENCE A 10, 1660–1669.
521 Liu, I., Lawton, L.A., Bahnemann, D.W., Liu, L., Proft, B., Robertson, P.K.J., 2009. The
522 photocatalytic decomposition of microcystin–LR using selected titanium dioxide materials.
523 Chemosphere 76, 549–553.
524 Liu, I., Lawton, L.A., Robertson, P.K.J., 2003. Mechanistic Studies of the Photocatalytic Oxidation of
525 Microcystin–LR: An Investigation of Byproducts of the Decomposition Process. Environ. Sci.
526 Technol. 37, 3214–3219.
527 Liu, X., Chen, Z., Zhou, N., Shen, J., Ye, M., 2010. Degradation and detoxification of microcystin–
528 LR in drinking water by sequential use of UV and ozone. J. Environ. Sci. 22, 1897–1902.
529 Liu, Y., Ren, J., Wang, X., Fan, Z., 2016. Mechanism and reaction pathways for microcystin–LR
530 degradation through UV/H_2O_2 treatment. PLoS ONE 11.
531 Llana–Ruiz–Cabello, M., Jos, A., Cameán, A., Oliveira, F., Barreiro, A., Machado, J., Azevedo, J.,
532 Pinto, E., Almeida, A., Campos, A., Vasconcelos, V., Freitas, M., 2019. Analysis of the Use of
533 Cylindrospermopsin and/or Microcystin–Contaminated Water in the Growth, Mineral Content, and
534 Contamination of *Spinacia oleracea* and *Lactuca sativa*. Toxins 11, 624.
535 Mohamed, Z.A., Bakr, A., 2018. Concentrations of cylindrospermopsin toxin in water and tilapia fish
536 of tropical fishponds in Egypt, and assessing their potential risk to human health. Environ. Sci.
537 Pollut. Res. 25, 36287–36297.
538 Moura, A.N., AragãO–Tavares, N.K.C., Amorim, C.A., 2018. Cyanobacterial blooms in freshwater
539 bodies from a semiarid region, northeast Brazil: A review. J. Limnol. 77, 179–188.
540 Peláez, M., de la Cruz, A.A., O'Shea, K., Falaras, P., Dionysiou, D.D., 2011. Effects of water
541 parameters on the degradation of microcystin–LR under visible light–activated TiO_2 photocatalyst.
542 Water Res. 45, 3787–3796.
543 Pestana, C.J., Hobson, P., Robertson, P.K.J., Lawton, L.A., Newcombe, G., 2020. Removal of
544 microcystins from a waste stabilisation lagoon: Evaluation of a packed–bed continuous flow TiO_2
545 reactor. Chemosphere 245, 125575.

Pignatello, J.J., Oliveros, E., MacKay, A., 2006. Advanced Oxidation Processes for Organic Contaminant Destruction Based on the Fenton Reaction and Related Chemistry. Crit. Rev. Environ. Sci. Technol. 36, 1–84.
Pineda–Mendoza, R.M., Briones–Roblero, C.I., Gonzalez–Escobedo, R., Rivera–Orduña, F.N., Martínez–Jerónimo, F., Zúñiga, G., 2020. Seasonal changes in the bacterial community structure of three eutrophicated urban lakes in Mexico city, with emphasis on *Microcystis spp*. Toxicon 179, 8–20.
Pinho, L.X., Azevedo, J., Brito, Â., Santos, A., Tamagnini, P., Vilar, V.J.P., Vasconcelos, V.M., Boaventura, R.A.R., 2015a. Effect of TiO_2 photocatalysis on the destruction of *Microcystis aeruginosa* cells and degradation of cyanotoxins microcystin–LR and cylindrospermopsin. Chem. Eng. J. 268, 144–152.
Pinho, L.X., Azevedo, J., Miranda, S.M., Ângelo, J., Mendes, A., Vilar, V.J.P., Vasconcelos, V., Boaventura, R.A.R., 2015b. Oxidation of microcystin–LR and cylindrospermopsin by heterogeneous photocatalysis using a tubular photoreactor packed with different TiO_2 coated supports. Chem. Eng. J. 266, 100–111.
Pinho, L.X., Azevedo, J., Vasconcelos, V.M., Vilar, V.J.P., Boaventura, R.A.R., 2012. Decomposition of *Microcystis aeruginosa* and Microcystin–LR by TiO_2 Oxidation Using Artificial UV Light or Natural Sunlight. J. Adv. Oxid. Technol. 15, 98.
Rezaei, M., rashidi, F., Royaee, S.J., Jafarikojour, M., 2014. Performance evaluation of a continuous flow photocatalytic reactor for wastewater treatment. Environ. Sci. Pollut. Res. 21, 12505–12517.
Rzymski, P., Poniedziałek, B., 2014. In search of environmental role of cylindrospermopsin: A review on global distribution and ecology of its producers. Water Res. 66, 320–337.
Sahel, K., Elsellami, L., Mirali, I., Dappozze, F., Bouhent, M., Guillard, C., 2016. Hydrogen peroxide and photocatalysis. Appl. Catal. B: Environ. 188, 106–112.
Scholz, S.N., Esterhuizen–Londt, M., Pflugmacher, S., 2017. Rise of toxic cyanobacterial blooms in temperate freshwater lakes: causes, correlations and possible countermeasures. Toxicol. Environ. Chem. 99, 543–577.
Sharma, V.K., Triantis, T.M., Antoniou, M.G., He, X., Peláez, M., Han, C., Song, W., O'Shea, K.E., de la Cruz, A.A., Kaloudis, T., Hiskia, A., Dionysiou, D.D., 2012. Destruction of microcystins by conventional and advanced oxidation processes: A review. Sep. Purif. Technol. 91, 3–17.
Skillen, N., Adams, M., McCullagh, C., Ryu, S.Y., Fina, F., Hoffmann, M.R., Irvine, J.T.S., Robertson, P.K.J., 2016. The application of a novel fluidised photo reactor under UV–Visible and natural solar irradiation in the photocatalytic generation of hydrogen. Chem. Eng. J. 286, 610–621.
Spoof, L., Catherine, A., 2017. Appendix 3: Tables of Microcystins and Nodularins, Handbook of Cyanobacterial Monitoring and Cyanotoxin Analysis. John Wiley and Sons Ltd., Chichester, UK, pp. 526–537.
Srikanth, B., Goutham, R., Badri Narayan, R., Ramprasath, A., Gopinath, K.P., Sankaranarayanan, A.R., 2017. Recent advancements in supporting materials for immobilised photocatalytic applications in waste water treatment. J. Environ. Manage. 200, 60–78.
Svirčev, Z., Lalić, D., Bojadžija Savić, G., Tokodi, N., Drobac Backović, D., Chen, L., Meriluoto, J., Codd, G.A., 2019. Global geographical and historical overview of cyanotoxin distribution and cyanobacterial poisonings. Arch. Toxicol. 93, 2429–2481.
Szlag, D.C., Sinclair, J.L., Southwell, B., Westrick, J.A., 2015. Cyanobacteria and Cyanotoxins Occurrence and Removal from Five High–Risk Conventional Treatment Drinking Water Plants. Toxins 7, 2198–2220.
USEPA, 2015. Drinking Water Health Advisories for Two Cyanobacterial Toxins. https://www.epa.gov/cyanohabs/epa-drinking-water-health-advisories-cyanotoxins; accessed 04 June 2020)
Wei, H., Wang, S., Xu, E.G., Liu, J., Li, X., Wang, Z., 2020. Synergistic toxicity of microcystin–LR and Cu to zebrafish (*Danio rerio*). Sci. Total Environ. 713, 136393.
WHO, 2011. Guidelines for drinking–water quality, fourth edition. WHO, p. 564.
Wiegand, C., Pflugmacher, S., 2005. Ecotoxicological effects of selected cyanobacterial secondary metabolites a short review. Toxicol. Appl. Pharmacol. 203, 201–218.

Xing, Z., Zhang, J., Cui, J., Yin, J., Zhao, T., Kuang, J., Xiu, Z., Wan, N., Zhou, W., 2018. Recent advances in floating TiO_2–based photocatalysts for environmental application. Appl. Catal. B: Environ. 225, 452–467.

Xu, Y., Langford, C.H., 2000. Variation of Langmuir adsorption constant determined for TiO_2–photocatalyzed degradation of acetophenone under different light intensity. J. Photochem. Photobio. A: Chem. 133, 67–71.

Yang, B., Park, H.-D., Hong, S.W., Lee, S.-H., Park, J.-A., Choi, J.-W., 2020. Photocatalytic degradation of microcystin-LR and anatoxin-a with presence of natural organic matter using UV-light emitting diodes/TiO_2 process. J. Water Process Eng. 34, 101163.

Zhang, G., Wurtzler, E.M., He, X., Nadagouda, M.N., O'Shea, K., El-Sheikh, S.M., Ismail, A.A., Wendell, D., Dionysiou, D.D., 2015. Identification of TiO_2 photocatalytic destruction byproducts and reaction pathway of cylindrospermopsin. Appl. Catal. B: Environ. 163, 591-598.

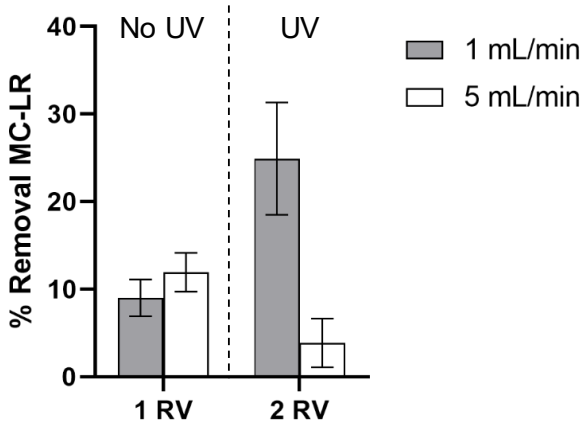

612
613 Figure 1. Effect of flow rate (1 and 5 mL/min) on the removal of microcystin-LR (MC-LR) in
614 a lab-scale flow through immobilized photocatalytic reactor. RV: reactor volume; UV:
615 ultraviolet. Data is presented as mean values and SD of n=3
616

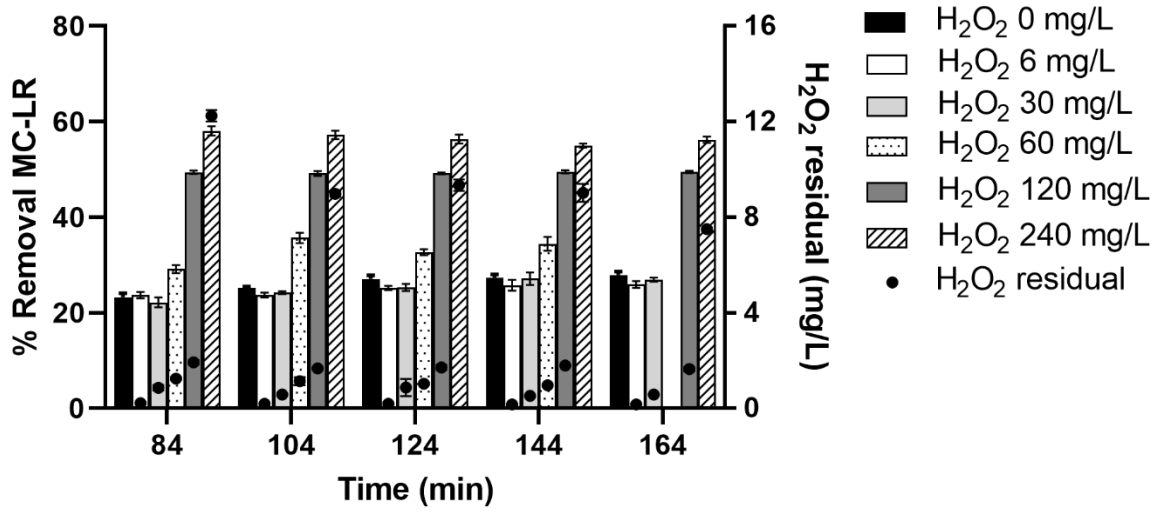

617

618 Figure 2. Effect of the concentration of H_2O_2 (0, 6, 30, 60, 120, 240 mg/L) on the removal of
619 microcystin-LR (MC-LR) at 1 mL/min in a lab-scale flow through immobilized
620 photocatalytic reactor at 84 (1 residence volume), 104, 124, 144 and 164 min. Concentration
621 of H_2O_2 residual at 84, 104, 124, 144 and 164 min. Data is presented as mean values and SD
622 of n=3.

623

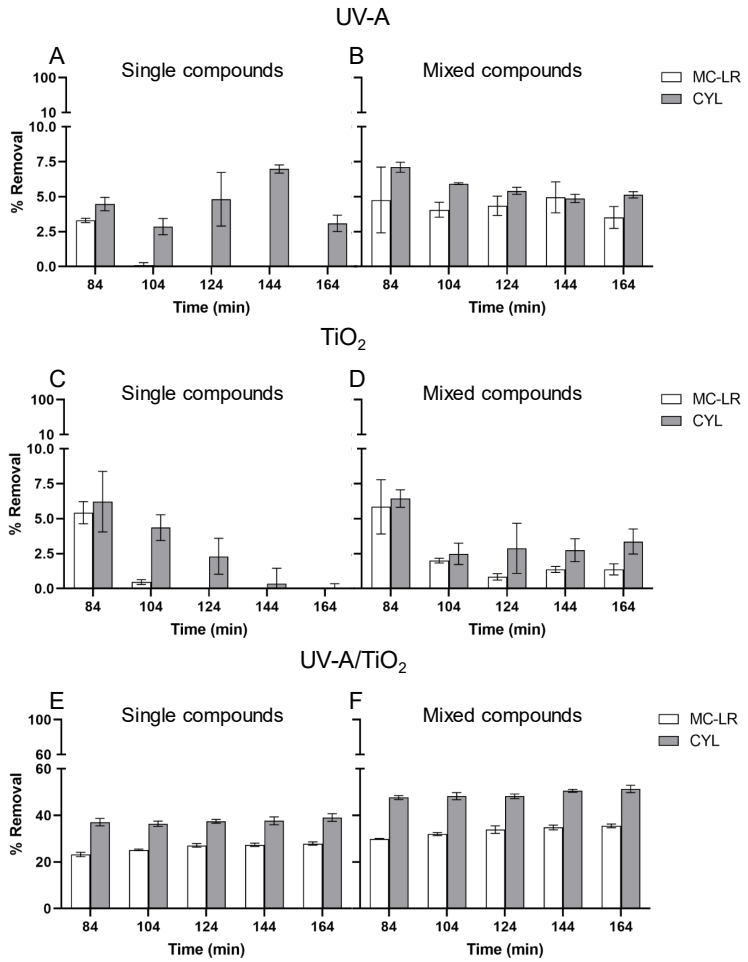

Figure 3. Effect of photolysis (UV-A), physical adsorption (TiO_2) and photocatalysis (UV-A/TiO_2) on the removal of microcystin-LR (MC-LR, 3 µg/mL), cylindrospermopsin (CYN, 3 µg/mL) and a mixed solution of MC-LR (1.5 µg/mL) and CYN (1.5 µg/mL) at 1 mL/min in a lab-scale flow through immobilized photocatalytic reactor at 84 (1 reactor volume), 104, 124, 144 and 164 min. Data is presented as mean values and SD of n=3.

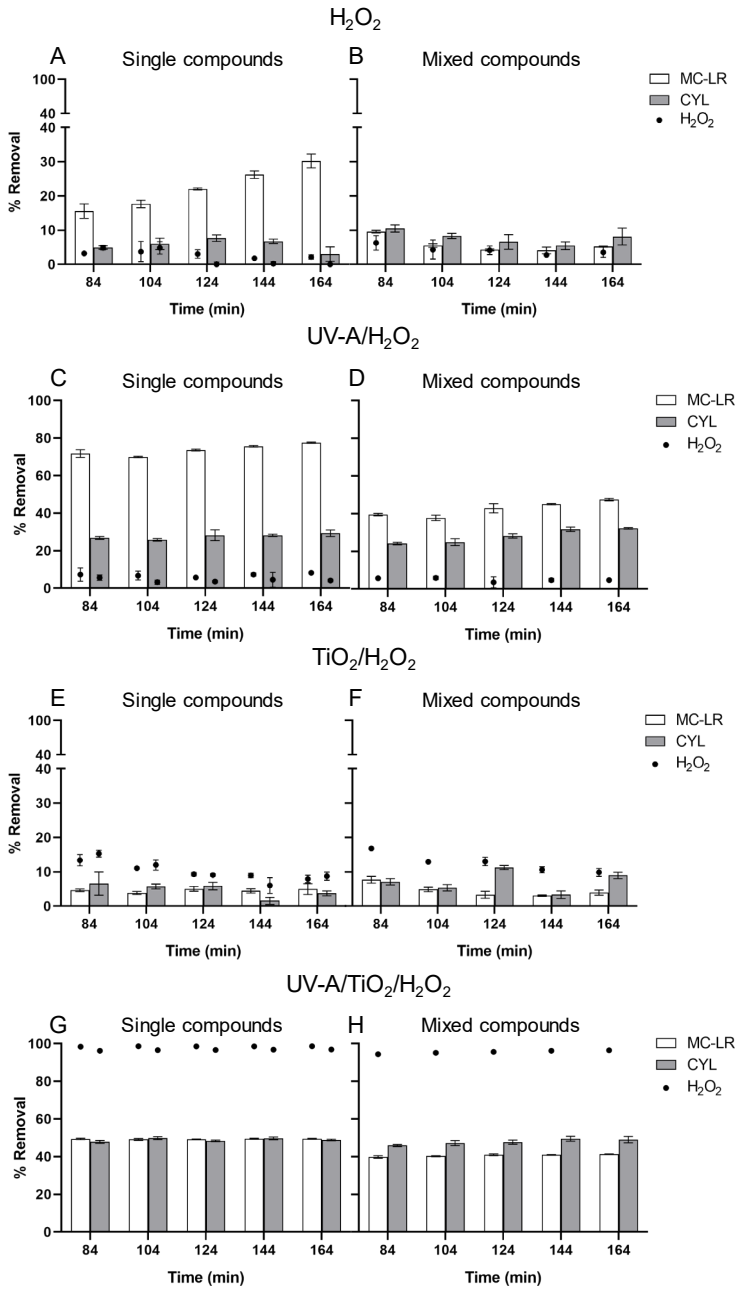

630

631 Figure 4. Effect of H_2O_2 oxidation, H_2O_2-assisted photolysis (UV-A/H_2O_2), H_2O_2-assisted
632 physical adsorption (TiO_2/H_2O_2) and H_2O_2-assisted photocatalysis (UV-A/TiO_2/H_2O_2) on the
633 removal of microcystin-LR (MC-LR, 3 µg/mL), cylindrospermopsin (CYN, 3 µg/mL) and a
634 mixed solution of MC-LR (1.5 µg/mL) and CYN (1.5 µg/mL) at 1 mL/min in a lab-scale
635 flow through immobilized photocatalytic reactor at 84 (1 reactor volume), 104, 124, 144 and
636 164 min. Data is presented as mean values and SD of n=3.

637

638

SUPPLEMENTARY MATERIAL

Degradation of microcystin-LR and cylindrospermopsin by continuous flow UV-A photocatalysis over immobilised TiO_2

Dolores Camacho-Muñoz[a*], Anne-Sophie Fervers[a], Carlos J. Pestana[a], Christine Edwards[a], Linda A. Lawton[a]

[a]School of Pharmacy and Life Sciences, Robert Gordon University, Aberdeen, AB10 7GJ, UK

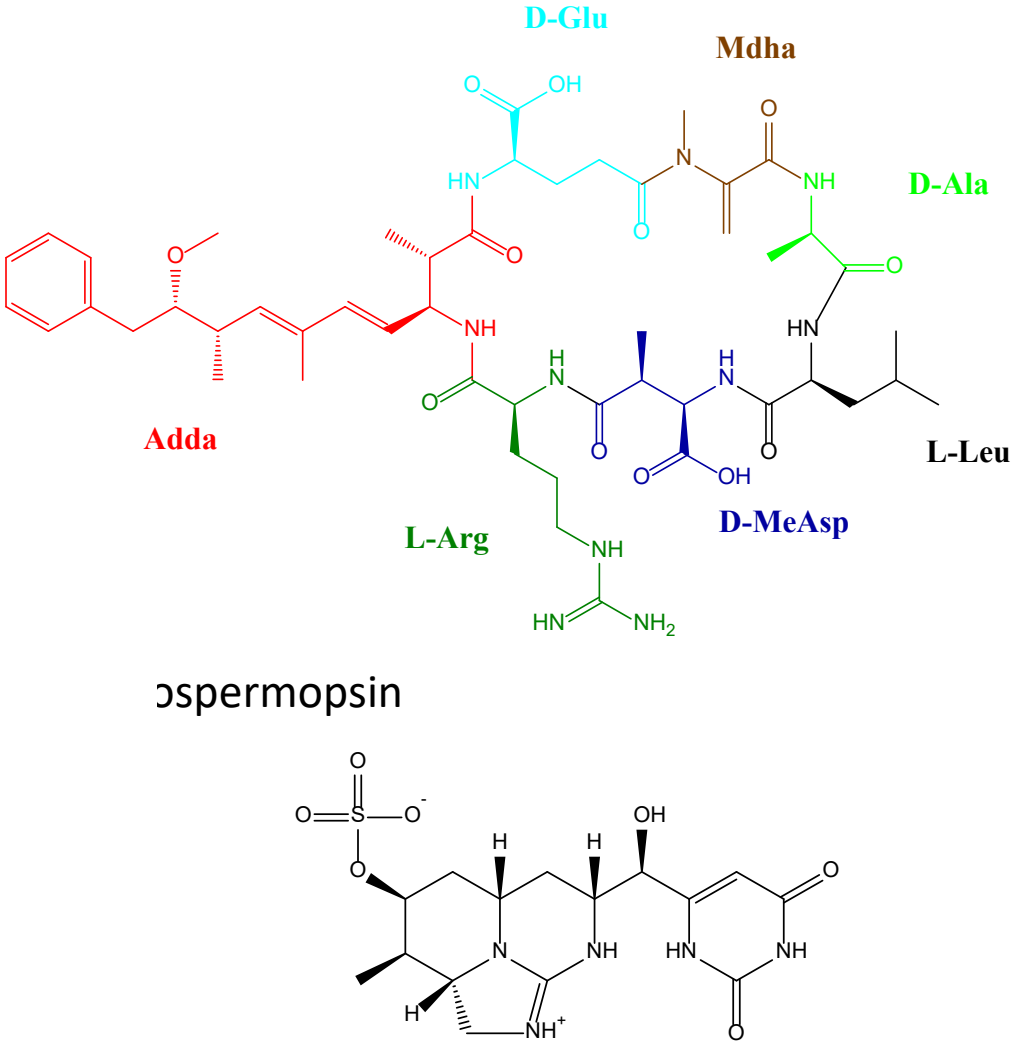

649

650 Figure S1. Chemical structure of microcystin-LR and cylindrospermopsin.

651

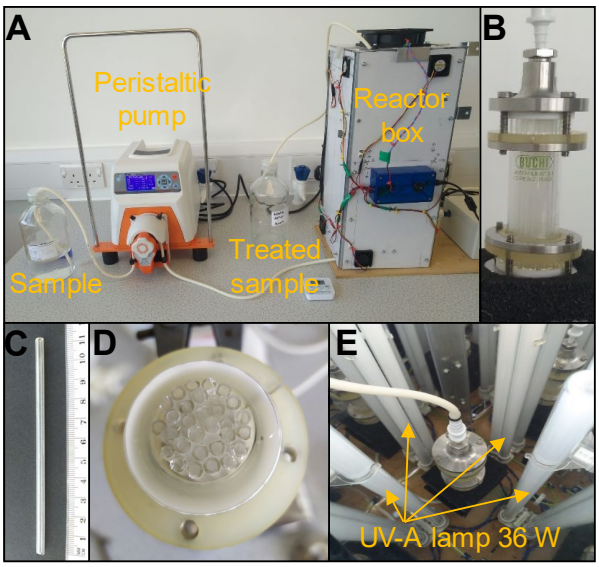

Figure S2. (A) Set up of the lab-scale flow through immobilized photocatalytic reactor; (B) Reactor vessel; (C) TiO_2 coated glass tube; (D) Packing of the TiO_2 coated glass tubes inside the reactor vessel; (E) Top view of the inside of the reactor box.

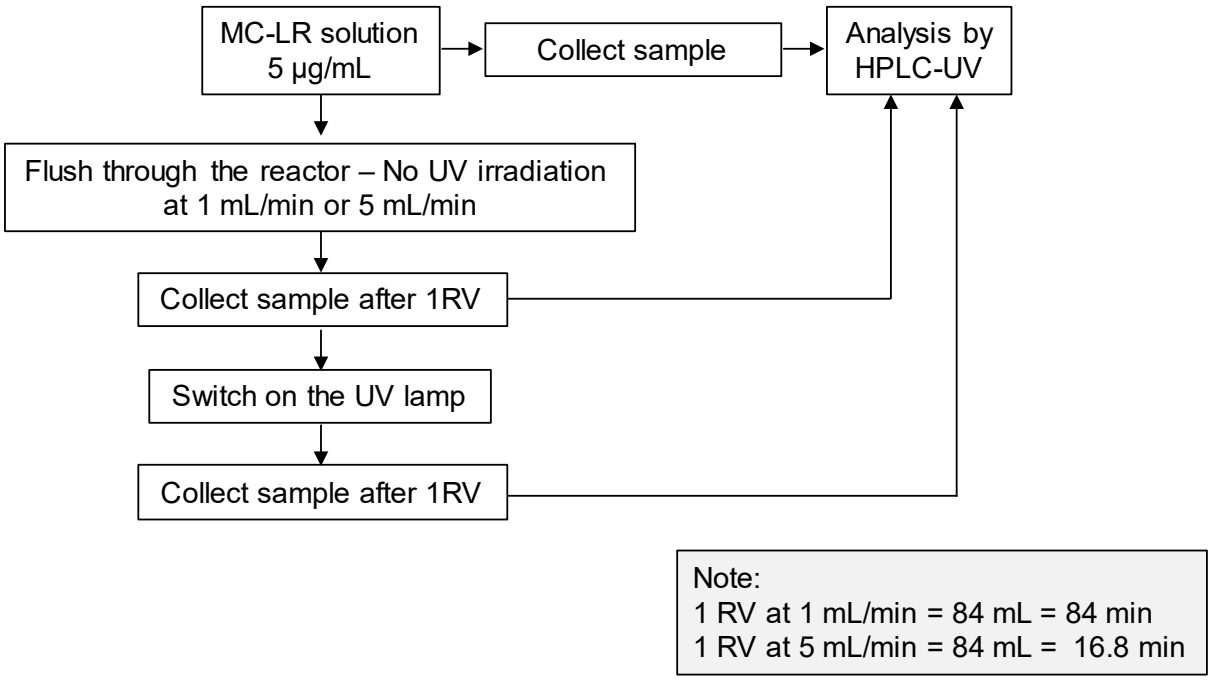

657

658 Figure S3. Flowchart to evaluate the effect of flow rate on the degradation of microcystin-LR

659 (MC-LR). RV: reactor volume; UV: ultraviolet.

660

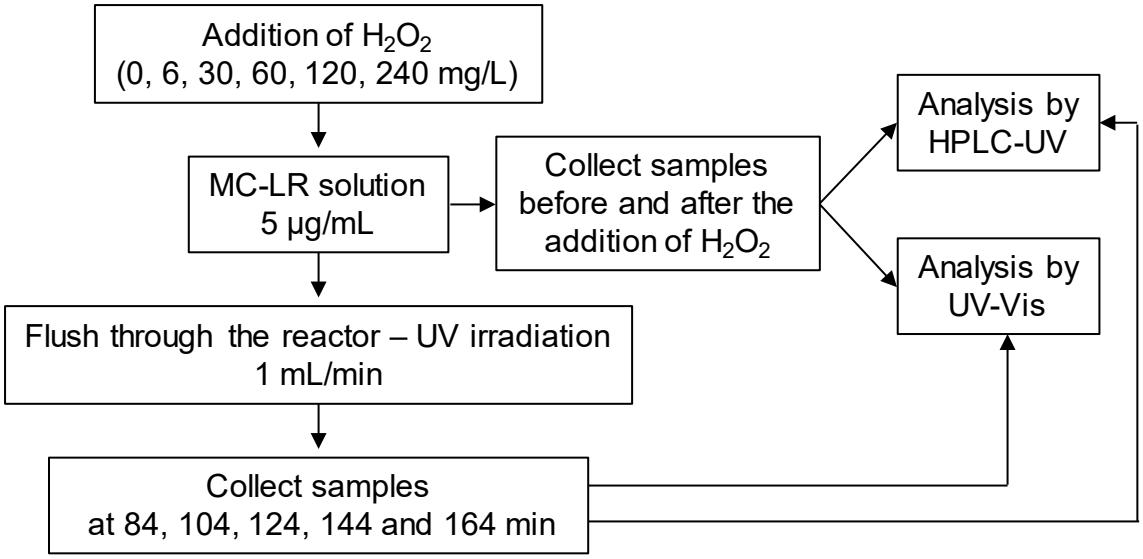

661

662 Figure S4. Flowchart to evaluate the effect of H_2O_2 (0, 6, 30, 60, 120 and 240 mg/L) on the

663 degradation of microcystin-LR (MC-LR). UV: ultraviolet.

664

Table S1. Summary of experimental conditions evaluated in this study

Experimental conditions	**UV-A**	**TiO_2**	**H_2O_2**
UV-A	x	-	-
TiO_2	-	x	-
UV-A/TiO_2	x	x	-
H_2O_2	-	-	x
UV-A/H_2O_2	x	-	x
TiO_2/H_2O_2	-	x	x
UV-A/TiO_2/H_2O_2	x	x	x